Vol. 18 (2026): Proceedings of 2026 International Conference on Smart Healthcare and Biomedical Engineering (ICSHBE 2026)
E-ISSN: 3105-0522 P-ISSN: 3105-0514
DOI: https://doi.org/10.70267/shbe.20268895

Early Diagnosis and Classification of Alzheimer's Disease Based on EEG Time–Frequency Images

Yuxuan Qi*

School of Biotechnology, East China University of Science and Technology, Shanghai 200030, China

**Corresponding author: Yuxuan Qi.*

Abstract

Mild cognitive impairment (MCI) is a cognitive disorder characterized by memory impairment and is associated with an increased risk of progression to Alzheimer's disease (AD). Therefore, classification of MCI and different stages of AD is fundamental for understanding and treating this disease. This study aims to provide an efficient and clinically deployable technical approach for EEG-based early auxiliary diagnosis of AD. In this work, multichannel resting-state electroencephalography (EEG) signals were transformed into time–frequency images, and a lightweight convolutional neural network (CNN) was constructed for three-class classification of AD, MCI, and healthy controls (HC). The proposed model achieved an accuracy of 84.96%, an F1-score of 0.8486, and a macro-average area under the curve (AUC) of 0.965 on the randomly split test set, significantly outperforming conventional machine learning approaches. These results demonstrate the feasibility of using EEG for early AD detection. From a practical perspective, the proposed intelligent EEG diagnostic framework shows potential for deployment in primary healthcare institutions and may provide theoretical support for addressing the growing challenges of AD diagnosis and treatment in the context of global population aging.

Keywords

Alzheimer's disease, mild cognitive impairment, quantitative electroencephalography, convolutional neural network, deep learning

1. Introduction

Alzheimer's disease (AD) is the most common neurodegenerative disorder and is primarily characterized by progressive cognitive decline and impairment in activities of daily living [1]. According to estimates from the World Health Organization, more than 55 million people worldwide are currently living with dementia, and this number is projected to exceed 150 million by 2050 [2]. Among these cases, AD accounts for approximately 60%–70%, imposing a substantial burden on families and society. Mild cognitive impairment (MCI), as the prodromal stage of AD, exhibits an annual conversion rate of approximately 10%–15% to AD, whereas the conversion rate among cognitively normal older adults is only 1%–2%. It is widely recognized that the pathophysiological alterations of AD begin long before the onset of clinical symptoms [3]. Once the disease progresses to the dementia stage, therapeutic efficacy becomes limited. Therefore, achieving early diagnosis during the MCI stage is of considerable clinical significance and urgency.

At present, traditional neuropsychological assessment relies primarily on laboratory-based neuropsychological examinations and clinical evaluations, such as the Mini-Mental State Examination (MMSE) and Common Objects Memory Test (COMT) [4]. However, such assessments require experienced clinicians and comprehensive testing procedures, which increase diagnostic subjectivity and variability. Although magnetic resonance imaging (MRI) and positron emission tomography (PET) can assist in evaluating pathological processes, their high cost and limited accessibility restrict widespread clinical application. Electroencephalography (EEG), by contrast, offers millisecond-level temporal resolution and is portable, low-cost, and noninvasive, making it a promising alternative to PET. Nevertheless, existing studies remain limited in data representation strategies. Most previous work either combines multichannel EEG signals into a unified representation or utilizes only single-channel recordings, thereby neglecting valuable spatial topological information and constraining the discriminative capability of classification models.

To address these limitations, this study proposes a deep learning-based classification framework using multichannel EEG time–frequency images. Specifically, 16-channel resting-state EEG signals are directly transformed into multichannel time–frequency images, which are subsequently used as input to a lightweight convolutional neural network (CNN) for three-class classification. Compared with conventional methods that rely on handcrafted feature engineering, the proposed framework offers advantages including end-to-end learning, richer feature representation, and convenient clinical deployment. This study provides methodological support for deep learning-based representation of multichannel EEG time–frequency features. Moreover, the proposed low-cost and noninvasive intelligent diagnostic framework demonstrates potential for implementation in primary healthcare institutions and may facilitate large-scale early screening of AD

2. Methods

Electroencephalography (EEG) is a neurophysiological measurement technique that records excitatory and inhibitory postsynaptic potentials of cortical pyramidal neurons using electronic instruments. EEG signals are typically divided into several frequency bands, including delta (0.5–4 Hz), theta (4–8 Hz), alpha (8–13 Hz), beta (13–30 Hz), and gamma (30–40 Hz). The alpha band can be further subdivided into alpha1 (8–10.5 Hz) and alpha2 (10.5–13 Hz), while the beta band can be subdivided into beta1 (13–20 Hz) and beta2 (20–30 Hz) [5-7]. Previous studies have shown that EEG characteristics in patients with AD and mild cognitive impairment (MCI) are primarily manifested as increased slow-wave power (delta and theta), decreased fast-wave power (alpha and beta), and anterior migration of alpha oscillations from the normal posterior occipital region toward the frontal cortex. The degree of EEG abnormality in MCI patients is generally intermediate between that of AD patients and healthy controls [7]. In addition, previous studies have suggested that EEG spectrogram images may effectively predict the progression from MCI to AD dementia [8].

2.1 Subjects and Data Acquisition

A total of 24 subjects were enrolled in this study and divided into three groups following clinical evaluation, including AD, MCI, and healthy control (HC), with 8 subjects in each group. Resting-state eyes-closed EEG data were collected from all participants. EEG recordings were acquired using a 16-channel EEG acquisition device. The recording duration for each subject was approximately 60 min.

2.2 Data Preprocessing and Generation of Multichannel Time–Frequency Images

The primary objective of data preprocessing was to transform the raw high-dimensional time–frequency signal streams into standardized image formats suitable for CNN processing. First, EDF files were loaded, all non-EEG channels were removed, and time–frequency data from 16 EEG channels were extracted. Subsequently, the data were segmented using non-overlapping sliding windows with a step size of 500. The time–frequency matrix (14×500) of each channel within each window was resized to 32×32 pixels, thereby generating multichannel images with dimensions of $32 \times 32 \times 16$. Finally, Z-score normalization was independently applied to each channel of each sample, resulting in a total of 35,598 processed samples.

2.3 Convolutional Neural Network Architecture

To process the generated multichannel time–frequency images, a lightweight yet structurally complete CNN model was designed in this study. The core design principle was to maintain effective feature extraction capability while preventing overfitting through adequate regularization, thereby accommodating the moderate sample size of the dataset. The overall architecture is illustrated in *Figure 1: Schematic diagram of CNN structure*.

Figure 1: Schematic diagram of CNN structure

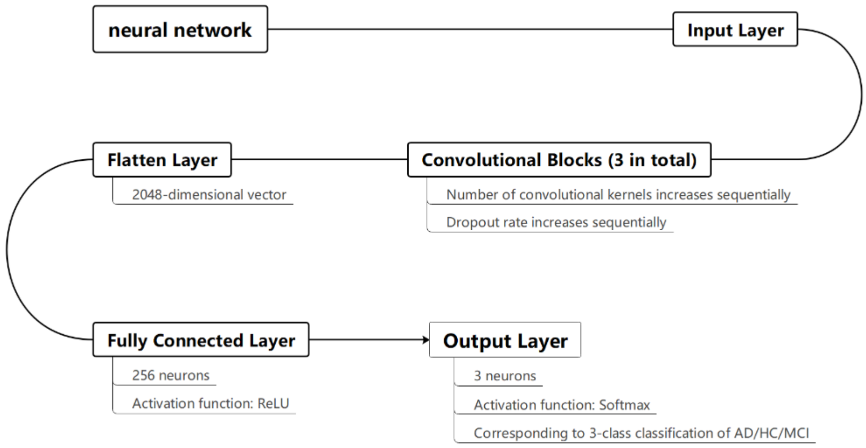

Each convolutional block consists of a two-dimensional convolutional layer (Conv2D) with a 3 × 3 kernel for capturing local time–frequency patterns. The number of filters increases progressively across blocks (32, 64, and 128) to enable hierarchical extraction of increasingly complex and abstract features. Each block further includes a batch normalization layer to accelerate convergence and improve training stability, a ReLU activation function, and a max-pooling layer with a 2 × 2 pooling window for downsampling. Dropout layers are also incorporated, with dropout rates of 0.25, 0.35, and 0.45, respectively, increasing with network depth to randomly deactivate neurons and encourage the model to learn more robust representations.

Following the convolutional blocks, a flatten layer converts the three-dimensional feature maps into a one-dimensional feature vector. A fully connected layer containing 256 neurons is then applied using ReLU activation, together with L2 weight regularization (coefficient = 0.001) to constrain model complexity. An additional dropout layer with a dropout rate of 0.5 is used as a key regularization strategy for the fully connected layer. Finally, the output layer contains three neurons corresponding to the AD, MCI, and HC classes, and employs the Softmax activation function to generate class prediction probabilities.

The model was trained using the Adam optimizer, with the initial learning rate determined through hyperparameter tuning, and categorical cross-entropy was employed as the loss function.

2.4 Experimental Design and Evaluation Strategy

2.4.1 Hyperparameter Tuning

To determine the optimal model configuration, controlled hyperparameter scanning experiments were conducted in this study. For the learning rate experiments, the dropout rate of the fully connected layer was fixed at 0.5, while the tested learning rate values were set to {0.001, 0.0003, 0.0001}. For the dropout experiments, the learning rate was fixed at 0.001, and the tested dropout values for the fully connected layer were set to {0.3, 0.5}. All experiments employed an early stopping strategy by monitoring validation loss, with the patience parameter set to 15 epochs. The best model weights were restored to prevent overfitting.

2.4.2 Dual Data Splitting and Evaluation Strategy

To comprehensively evaluate model performance, two distinct data partitioning strategies were adopted in this study.

The first strategy was random sample splitting (conventional evaluation), in which all 35,598 samples were randomly shuffled and divided into training and test sets at a ratio of 0.8:0.2. Subsequently, 15% of the training set was further allocated as a validation set for hyperparameter tuning and early stopping.

The second strategy was subject-wise stratified splitting (generalization evaluation), in which the 24 subjects were divided at an approximate ratio of 0.7:0.3. Specifically, all samples from 16 subjects were used for training, while all samples from the remaining 8 previously unseen subjects were reserved for testing. This strategy strictly simulates real-world clinical scenarios in which a model trained on existing patient data is used to diagnose entirely new patients. It is regarded as the gold standard for evaluating clinical applicability and generalization performance.

2.4.3 Evaluation Metrics

For the test sets under both partitioning strategies, performance was evaluated using Accuracy, Precision, Recall, and F1-score. Receiver operating characteristic (ROC) curves were plotted, and the area under the curve (AUC) was calculated for each class, together with macro-average, micro-average, and weighted-average AUC values. In addition, confusion matrices were generated to visually illustrate the distribution of classification errors across categories.

All experiments were conducted under identical hardware and software environments to ensure comparability of the results.

3. Results

3.1 Hyperparameter Tuning Results

The hyperparameter tuning experiments indicate that, under the data and model architecture used in this study, the impact of hyperparameters on the final validation accuracy is relatively moderate. The results are shown in Table 1.

Table 1: Hyperparameter tuning results

Groups	Learning Rate	Dropout	Best Val Accuracy	Test Accuracy
1	0.001	0.5	0.9660	0.9643
2	0.0003	0.5	0.9670	0.9607
3	0.0001	0.5	0.9656	0.9605
4	0.001	0.3	0.9691	0.9636
5	0.001	0.3	0.9658	0.9600

For learning rate selection, experimental results showed that when the learning rate was set to 0.001, the model achieved the best overall performance, with faster convergence and higher validation accuracy. In contrast, smaller learning rates (0.0003 and 0.0001) led to slower convergence and slightly reduced performance. Therefore, 0.001 was selected as the optimal learning rate for subsequent experiments.

For dropout configuration, comparative experiments indicated that a dropout rate of 0.5 in the fully connected layer resulted in better generalization performance than a dropout rate of 0.3, effectively reducing overfitting while maintaining stable model training. Based on these results, the final model configuration adopted a learning rate of 0.001 and a dropout rate of 0.5.

3.2 Results under Random Sample Splitting

The CNN model achieved outstanding classification performance on the independent test set, as shown in table 2.

Under the random sample splitting strategy, the proposed model achieved strong classification performance across the three categories (AD, MCI, and HC). The overall classification accuracy reached 84.96%, with an F1-score of 0.8486 and a macro-average AUC of 0.965.

The confusion matrix in figure 2 clearly illustrates that most samples were correctly classified, with relatively few misclassifications occurring between adjacent categories (particularly between MCI and HC), which is consistent with their clinical similarity.

Table 2: Performance under random split

Metrics	Value
Accuracy	0.8496
Precision	0.8687
Recall	0.8295
F1-score	0.8486
Macro AUC	0.965

Figure 2: Confusion matrix

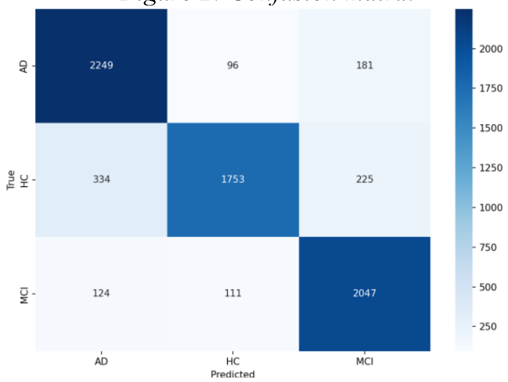

The ROC curves in Figure 3 further demonstrate that the model achieved high discriminative capability for all three classes, with consistently high AUC values. These results indicate that the proposed model is effective in extracting discriminative time–frequency features from multichannel EEG data under conventional evaluation settings.

3.3 Results under Subject-Wise Splitting

Under the more challenging subject-wise splitting strategy, the overall classification performance in *Table 3 performance under stratified split* showed a certain degree of decline compared with the random splitting scenario, reflecting the increased difficulty of generalizing to unseen subjects. However, the model still maintained relatively robust performance, demonstrating its generalization capability.

Table 3: Performance under stratified split

Metrics	Value
Accuracy	0.3876
Precision	0.3897
Recall	0.3800
F1-score	0.3848

Figure 3: ROC curves under random split

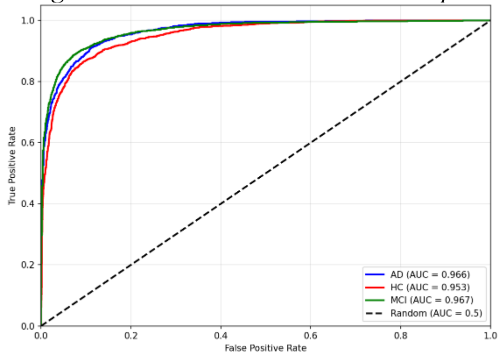

The confusion matrix clearly illustrates a higher degree of misclassification compared with the random splitting results, particularly between MCI and other groups. This phenomenon is expected, as inter-subject variability in EEG signals introduces additional complexity to the classification task.

Despite this performance reduction, the model continued to exhibit reasonable discriminative ability, indicating that the proposed framework retains practical potential for real-world clinical applications.

4. Discussion

4.1 Effectiveness of Multi-Channel Time–Frequency Image Representation and Its Clinical Application Potential

The multi-channel time–frequency image representation method proposed in this study demonstrates significant innovation and application value at both theoretical and practical levels. At the theoretical level, this method overcomes the paradigm limitations of traditional EEG feature engineering. Previous studies have confirmed spectral characteristics such as reduced alpha power in patients with Alzheimer's disease [9], yet their analyses rely on manually selected frequency band features, making it difficult to capture spatially coordinated patterns across multiple channels. Other studies have also identified theta power as an early marker of cognitive decline [10], but are similarly constrained by the limited representational capacity of single-band features.

In contrast, this study innovatively constructs multi-channel images directly from 16-channel time–frequency EEG data, enabling the convolutional neural network to learn temporal, spectral, and spatial distribution features in an end-to-end manner. At the practical level, compared with neuroimaging techniques such as MRI and PET, the proposed EEG-based intelligent diagnostic framework possesses significant advantages, including low cost, non-invasiveness, and portability. These characteristics indicate strong potential for large-scale early screening of AD and MCI.

4.2 Insights from the Dual Evaluation Strategy

One of the most valuable findings of this study arises from the comparison between the two evaluation strategies. Under random sample splitting, the model achieved an accuracy of 84.96% and a macro-averaged AUC of 0.965, demonstrating the technical effectiveness of the proposed framework. Its performance is competitive compared with existing EEG-based quantitative analysis methods [11-12].

Furthermore, the subject-wise stratified splitting strategy simulates a real clinical scenario, namely, "training on known patients and predicting unseen patients" which represents a critical requirement for any clinical decision-support system. Under this more stringent condition, the model still achieved performance significantly above the random baseline, indicating that the neurophysiological feature patterns learned from training subjects possess preliminary cross-subject transferability. This finding provides objective evidence supporting the clinical translation potential of this study.

Overall, these results strongly suggest that EEG-based intelligent early diagnosis of AD is practically feasible and holds important implications for the development of automated and low-cost early screening tools for cognitive impairment.

4.3 Future Perspectives

Although this study constructed a CNN model based on data from only 24 subjects, it has validated the feasibility of automatically distinguishing AD, MCI, and healthy controls using EEG time–frequency features, thereby providing a technical pathway for non-invasive and rapid early screening of AD. The model demonstrated strong performance under random splitting and maintained accuracy significantly above the three-class random baseline under stratified splitting, indicating preliminary generalization capability.

Based on these findings, future work can be pursued in two main directions. First, large-scale, multi-center clinical data collection should be conducted to substantially increase the number and diversity of subjects in the training set, thereby improving model accuracy, generalization ability, and robustness, and strengthening the foundation for clinical translation. Second, multimodal models integrating EEG functional features with structural MRI (sMRI) features can be developed to exploit complementary information, enhance diagnostic accuracy, and promote the clinical implementation of intelligent AD diagnostic systems.

5. Conclusions

This study innovatively transforms multi-channel EEG time–frequency data into image representations and employs a convolutional neural network for end-to-end learning. The results demonstrate that this paradigm outperforms traditional feature-based methods in the AD/MCI/HC three-class classification task, achieving an accuracy of approximately 85% and an AUC of 0.965, thereby confirming its efficient and effective feature extraction and classification capability.

Furthermore, through a rigorous subject-wise stratified splitting strategy, the model exhibits generalization performance above the random baseline when applied to entirely unseen individuals, demonstrating its potential for clinical application. At the same time, the findings reveal that inter-subject variability constitutes a key barrier limiting the practical deployment of the model.

Taken together, this study provides an automated and efficient technical pathway for EEG-based early screening of cognitive impairment. Future work will focus on expanding the dataset, optimizing the model, and improving interpretability. The integration of multimodal data may further enhance performance. With these improvements, the framework has the potential to evolve into a reliable clinical decision-support tool, contributing to address the challenges of Alzheimer's disease diagnosis and treatment in aging societies.

References

[1] Dementia and Cognitive Disorders Study Group of Chinese Medical Association Neurology Branch. (2024). Chinese expert consensus on the diagnosis and treatment of mild cognitive impairment due to Alzheimer's disease 2024. *Chinese Journal of Neurology*, *57*(7), 715–737.

[2] Scheltens, P., De Strooper, B., Kivipelto, M., Holstege, H., Chételat, G., Teunissen, C. E., Cummings, J., & van der Flier, W. M. (2021). Alzheimer's disease. *The Lancet*, 397(10284), 1577–1590. https://doi.org/10.1016/S0140-6736(20)32205-4

[3] Safiri, S., Amir, G. J., Fazlollahi, A., Morsali, S., Sarkesh, A., Amin, D. S., . . . Ali-Asghar Kolahi. (2024). Alzheimer's disease: A comprehensive review of epidemiology, risk factors, symptoms diagnosis, management, caregiving, advanced treatments and associated challenges. *Frontiers in Medicine, 11*, 1474043. https://doi.org/10.3389/fmed.2024.1474043

[4] Yang, L. (2023). *Quantitative electroencephalogram study of Alzheimer's disease-related cognitive impairment* [Master's thesis, University of Electronic Science and Technology of China]. https://doi.org/10.27005/d.cnki.gdzku.2023.005827.

[5] Lizio, R., Del Percio, C., Marzano, N., Soricelli, A., Yener, G. G., Başar, E., ... & Babiloni, C. (2015). Neurophysiological assessment of Alzheimer's disease individuals by a single electroencephalographic marker. *Journal of Alzheimer's disease*, *49*(1), 159-177.

[6] Babiloni, C., Visser, P. J., Frisoni, G., De Deyn, P. P., Bresciani, L., Jelic, V., ... & Nobili, F. (2010). Cortical sources of resting EEG rhythms in mild cognitive impairment and subjective memory complaint. *Neurobiology of Aging*, *31*(10), 1787-1798.

[7] Babiloni, C., Lizio, R., Del Percio, C., Marzano, N., Soricelli, A., Salvatore, E., ... & Rossini, P. M. (2013). Cortical sources of resting state EEG rhythms are sensitive to the progression of early stage Alzheimer's disease. *Journal of Alzheimer's Disease*, *34*(4), 1015-1035.

[8] Puri, D.V., Gawande, J.P., Kachare, P.H. *et al.* Optimal time-frequency localized wavelet filters for identification of Alzheimer's disease from EEG signals. *Cogn Neurodyn* 19, 12 (2025). https://doi.org/10.1007/s11571-024-10198-7

[9] Morabbi, F., & Keyvanpour, M. R. (2022). Efficient deep neural networks for classification of Alzheimer's disease and mild cognitive impairment. Cognitive Computation, 14(4), 1247–1265. https://doi.org/10.1007/s12559-021-09967-x

[10] Jiao, B., Li, R., Zhou, H., Qing, K., Liu, H., Pan, H., . . . Dong, Y. (2023). Neural biomarker diagnosis and prediction to mild cognitive impairment and Alzheimer's disease using EEG technology. Alzheimer's Research & Therapy, 15, 1-14. https://doi.org/10.1186/s13195-023-01181-1

[11] Musaeus, C. S., Engedal, K., Høgh, P., Jelic, V., Mørup, M., Naik, M., ... & Andersen, B. B. (2018). EEG theta power is an early marker of cognitive decline in dementia due to Alzheimer's disease. Journal of Alzheimer's Disease, 64(4), 1359-1371.

[12] Smailovic, U., & Jelic, V. (2019). Neurophysiological markers of Alzheimer's disease: quantitative EEG approach. *Neurology and therapy*, *8*(Suppl 2), 37-55.

Funding

This research received no external funding.

Conflicts of Interest

The authors declare no conflict of interest.

Acknowledgment

This paper is an output of the science project.

Open Access